BIOCHEMISTRY
including biophysical chemistry & molecular biology
Article

Biochemistry **2010,** *49,* 2227–2234 2227
DOI: 10.1021/bi901721u

Regulation of Actin Polymerization and Adhesion-Dependent Cell Edge Protrusion by the Abl-Related Gene (Arg) Tyrosine Kinase and N-WASp[†]

Matthew M. Miller,[‡] Stefanie Lapetina,[§] Stacey M. MacGrath,[§] Mindan K. Sfakianos,[§,#] Thomas D. Pollard,[‡,§,∥] and Anthony J. Koleske*[,§,⊥,@]

[‡]*Department of Cell Biology,* [§]*Department of Molecular Biophysics and Biochemistry,* [∥]*Department of Molecular, Cellular, and Developmental Biology,* [⊥]*Department of Neurobiology, and* [@]*Interdepartmental Neuroscience Program, Yale University, New Haven, Connecticut 06520.* [#]*Current address: Department of Cellular Regulation, Genentech Inc., South San Francisco, CA 94080.*

Received October 5, 2009; Revised Manuscript Received January 16, 2010

ABSTRACT: Extracellular cues stimulate the Abl family nonreceptor tyrosine kinase Arg to promote actin-based cell edge protrusions. Several Arg-interacting proteins are potential links to the actin cytoskeleton, but exactly how Arg stimulates actin polymerization and cellular protrusion has not yet been fully elucidated. We used affinity purification to identify N-WASp as a novel binding partner of Arg. N-WASp activates the Arp2/3 complex and is an effector of Abl. We find that the Arg SH3 domain binds directly to N-WASp. Arg phosphorylates N-WASp on Y256, modestly increasing the affinity of Arg for N-WASp, an interaction that does not require the Arg SH2 domain. The Arg SH3 domain stimulates N-WASp-dependent actin polymerization in vitro, and Arg phosphorylation of N-WASp weakly stimulates this effect. Arg and N-WASp colocalize to adhesion-dependent cell edge protrusions in vivo. The cell edge protrusion defects of *arg*−/− fibroblasts can be complemented by re-expression of an Arg-yellow fluorescent protein (YFP) fusion, but not by an N-WASp binding-deficient Arg SH3 domain point mutant. These results suggest that Arg promotes actin-based protrusions in response to extracellular stimuli through phosphorylation of and physical interactions with N-WASp.

Cellular locomotion, cell shape changes, and other important cellular processes require selective cell membrane protrusion in response to extracellular signaling cues. This protrusion is powered by localized actin polymerization. Morphogens, extracellular matrix molecules, or chemotactic factors stimulate cell surface receptors and trigger specific signaling cascades to activate proteins known as nucleation promoting factors (NPFs)[1] by overcoming autoinhibition or inhibitory factors (*1*, *2*). Active NPFs bind to the actin-related protein (Arp) 2/3 complex and promote its binding to the side of an existing actin filament, a reaction that allows the Arp2/3 complex to nucleate a new actin filament as a branch on the old filament (*3*, *4*). Actin filaments at the cell periphery are predominantly oriented with the growing barbed end toward the cell membrane, so an increased level of actin polymerization results in a pushing force against the inside of the cell membrane that drives the formation of protrusive structures (*5*).

Binding of the extracellular matrix protein fibronectin to integrins or platelet-derived growth factor (PDGF) to PDGF receptors activates intracellular signaling cascades that lead to the formation of actin-based cellular protrusions. Both pathways impinge on Arg, an Abl family nonreceptor tyrosine kinase, which mediates formation of actin-rich protrusions (*6*−*10*). The importance of Arg in these pathways has been described, and a number of the downstream targets of Arg signaling have been identified (*6*, *9*, *11*, *12*); however, the mechanism through which Arg affects actin polymerization and cellular protrusion has not yet been fully characterized. We previously reported that cortactin, a weak NPF, is a kinase substrate and binding partner of Arg (*9*, *13*), but it is unclear whether cortactin engagement is sufficient to promote actin polymerization or if other factors are required.

Here we identify the NPF N-WASp (*2*, *14*) as a potential effector of Arg. We show that the Arg SH3 domain binds directly to N-WASp and that the Arg SH3 domain activates N-WASp-dependent actin polymerization in vitro. Phosphorylation of N-WASp by Arg modestly enhances binding of the Arg SH3 domain to N-WASP and actin polymerization. We also demonstrate that Arg and N-WASp colocalize to adhesion-dependent cell protrusions and that Arg with a mutation that compromises binding to N-WASp is unable to support cell edge protrusion. Thus, Arg interacts with N-WASp through both binding and

[†]This work was supported by Public Health Service Grants NS39475 and CA133346 to A.J.K. and GM026338 to T.D.P. M.M.M. is supported by a National Research Service Award MSTP Training Grant (NIH MSTP TG 5T32GM07205). A.J.K. is an Established Investigator of the American Heart Association.

*To whom correspondence should be addressed. Phone: (203) 785-5624. Fax: (203) 785-7979. E-mail: anthony.koleske@yale.edu.

[1]Abbreviations: Arg, Abl-related gene; N-WASp, Neural-Wiskott Aldrich syndrome protein; NPF, nucleation promoting factor; Arp, actin-related protein; PDGF, platelet-derived growth factor; WBE, whole brain extract; SH3, Src homology 3; SH2, Src homology 2; SDS, sodium dodecyl sulfate; PAGE, polyacrylamide gel electrophoresis; MALDI-TOF, matrix-adsorbed laser desorption ionization time-of-flight; GST, glutathione *S*-transferase; β-ME, β-mercaptoethanol; pN-WASp, phosphorylated N-WASp; PCR, polymerase chain reaction; IPTG, isopropyl β-D-1-thiogalactopyranoside; DTT, dithiothreitol; EDTA, ethylenediaminetetraacetic acid; K_d, dissociation constant; K_M, Michaelis constant; WASp, Wiskott Aldrich syndrome protein; F-actin, filamentous actin; BSA, bovine serum albumin; EGTA, ethylene glycol bis(2-aminoethyl ether)-*N*,*N*,*N*′,*N*′-tetraacetic acid; YFP, yellow fluorescent protein; WT, wild type.

Published on Web 02/10/2010

phosphorylation events to stimulate N-WASp-dependent actin polymerization, pointing to this interaction as a mechanism through which Arg mediates stimulus-dependent actin-based protrusion.

EXPERIMENTAL PROCEDURES

Identification of Proteins That Interact with Arg. Whole adult mouse brains were homogenized in homogenization buffer (HB) [20 mM HEPES (pH 7.4), 25 mM potassium acetate, 320 mM sucrose, 1% Triton X-100, protease inhibitors (aprotinin, benzamidine, chymostatin, leupeptin, phenylmethanesulfonyl fluoride, and pepstatin A), and phosphatase inhibitors (sodium fluoride and sodium orthovanadate)] using 1.67 mL of HB/brain. The homogenate was incubated on ice for 30 min and centrifuged at 100000*g* for 1 h at 4 °C. The supernatant, or whole brain extract (WBE), was aliquoted and snap-frozen until it was used.

GST or GST-Arg-SH3SH2 coupled to glutathione agarose beads at 1 mg/mL was equilibrated with HB and added to WBE at a bead:WBE ratio of 1:100 by volume. The mixture was incubated with end-over-end rotation at 4 °C for 2 h, and beads were pelleted at 1000 rpm for 10 s. The beads were washed with HB for 3 × 5 min. Proteins were eluted from the beads by addition of an equal volume of 4× Laemmli sample buffer (*15*) and being boiled for 10 min, separated by SDS−PAGE using a 10% acrylamide gel, and visualized by Coomassie Brilliant Blue staining. Protein bands that were pulled down by GST-Arg-SH3SH2 but not by GST were excised from the acrylamide gel, subjected to trypsin digestion, and identified using MALDI-TOF mass spectrometry (*16*).

Molecular Cloning and Purification of Recombinant Proteins. Murine Arg and human N-WASp cDNA were cloned with an engineered His_6 tag into the pFastbac1 vector (Invitrogen). A His_6-tagged N-WASp(Y256F) construct was created using PCR-based mutagenesis. Protein was expressed using the Bac-to-Bac baculovirus expression system using a modification of a previously described protocol (*17*). Cells were lysed in detergent-containing lysis buffer [50 mM HEPES (pH 7.25), 5 mM β-ME, 500 mM KCl, 0.01% NP-40, 5% glycerol, 1% Triton, and protease inhibitors]. His_6-Arg was purified over an SP-Sepharose column, using a step salt gradient to elute, followed by a Ni affinity column, using ArgEB buffer [20 mM HEPES (pH 7.25), 5 mM β-ME, 500 mM KCl, 0.01% NP-40, 5% glycerol, 100 mM imidazole, and protease inhibitors] to elute. His_6-N-WASp and His_6-N-WASp(Y256F) were purified over a Ni affinity column using NWEB buffer (identical to ArgEB, but with 150 mM KCl) to elute.

Phosphorylated N-WASp (pN-WASp) was obtained via co-expression of untagged Arg and His_6-N-WASp in the same insect cell cultures and purification over a Ni affinity column following the same procedure outlined for unphosphorylated N-WASp. The phosphorylation status of N-WASp was verified by immunoblotting 30 ng of purified protein with a cocktail of anti-phosphotyrosine antibodies [4G10 (Upstate) and PY20 (Santa Cruz)]. Anti-N-WASp immunoblotting was performed as a loading control using anti-N-WASp rabbit antiserum from a rabbit immunized regularly with full-length N-WASp and adjuvant over a period of several months according to standard protocols.

PCR-based mutagenesis was used to clone Arg protein fragments and point mutants into pGEX-4T-1 (GE Healthcare) (the amino acid numbering corresponds to the myristoylated form of murine Arg): GST-Arg-SH3SH2, GST-Arg-SH3, GST-Arg-SH2, GST-Arg-SH3SH2(W145K), GST-Arg-SH3SH2(R198K), GST-Arg-SH3(W145K), and GST-Arg-SH2(R198K). PCR-based mutagenesis was also used to create a constitutively active GST-Cdc42(G12V) construct from a GST-Cdc42 construct in pGEX-2TK. The GST-tagged proteins were all expressed in *Escherichia coli* using 0.5 mM IPTG and overnight incubation at 26 °C. Bacteria were lysed at 4 °C in lysis buffer [20 mM Tris (pH 8.0), 1 mM DTT, 150 mM KCl, 2 mM EDTA, and protease inhibitors] using a French press. The lysate was clarified by being spun at 100000*g* for 30 min and purified over a glutathione agarose column, using glutathione elution buffer [20 mM Tris (pH 8.0), 1 mM DTT, 150 mM KCl, 2 mM EDTA, and 10 mM glutathione] to elute. The proteins were buffer exchanged over a Sephadex G-25 column into NWEB.

Determination of Binding Affinity. Arg was immobilized on Affigel 10 beads (Bio-Rad) according to the manufacturer's directions, and GST-tagged Arg fragments and mutants were bound to glutathione agarose beads at a concentration of 20 μM (moles of protein per volume of beads). We assessed binding by mixing 20 μL of beads in NWEB with 500 μL of NWEB containing a range of concentrations of N-WASp, giving a final Arg concentration of 0.8 μM (moles of protein per volume of reaction mixture). These binding reaction mixtures were mixed by end-over-end rotation for 30 min at 4 °C. The beads were washed quickly with binding buffer (NWEB), and bound proteins were eluted from the beads with 4× LSB, resolved by SDS−PAGE, and visualized by Coomassie Brilliant Blue staining. Gels were scanned on an ImageQuant densitometer (Bio-Rad), and protein bands were quantitated using Quantity One (Bio-Rad). The data were plotted and fit to a binding isotherm, and K_d values were determined using Prism (GraphPad).

Kinase Assays. Kinase assays were performed as previously described (*9*, *17*) with Arg and N-WASp or cortactin in the absence and presence of constitutively active GST-Cdc42(G12V), actin, and the Arp2/3 complex.

Actin Polymerization Assays. Native bovine Arp2/3 complex was purified from bovine calf thymus using a modification of a previously described protocol (*18*). Native monomeric actin was purified from chicken skeletal muscle as described previously (*18*−*20*). A portion of the actin monomers were labeled with pyrenyliodoacetamide (*20*, *21*). Actin polymerization assays were performed and barbed end concentrations calculated as previously described (*22*).

Cell Culture and Retroviral Expression. Wild-type (WT) and *arg*−/− cells were maintained as previously described (*8*). The ArgW145K point mutation was introduced by PCR and site-directed mutagenesis using murine type IV myristoylated Arg as a template. The sequence was cloned into N1-EYFP (Clontech Laboratories, Inc.). The tagged sequence was then subcloned into retroviral expression vector PK1 (a gift from A. M. Pendergast, Duke University, Durham, NC). mCherry was cloned in frame to human N-WASp, and the mCherry-N-WASp fusion was cloned into the pLXSN retrovirus (Clontech, Inc.). Retrovirus and reconstituted cell lines were generated as described previously (*8*, *13*), and Arg/Arg(W145K)-YFP expression levels were determined by quantitative immunoblotting using wild-type fibroblast extracts and purified recombinant Arg as standards. Arg-YFP and Arg(W145K)-YFP were expressed in reconstituted cells at 2.0- and 2.5-fold endogenous levels, respectively.

Fluorescence Microscopy. For colocalization experiments, FACS-sorted *arg*−/− + Arg-YFP fibroblasts were infected with

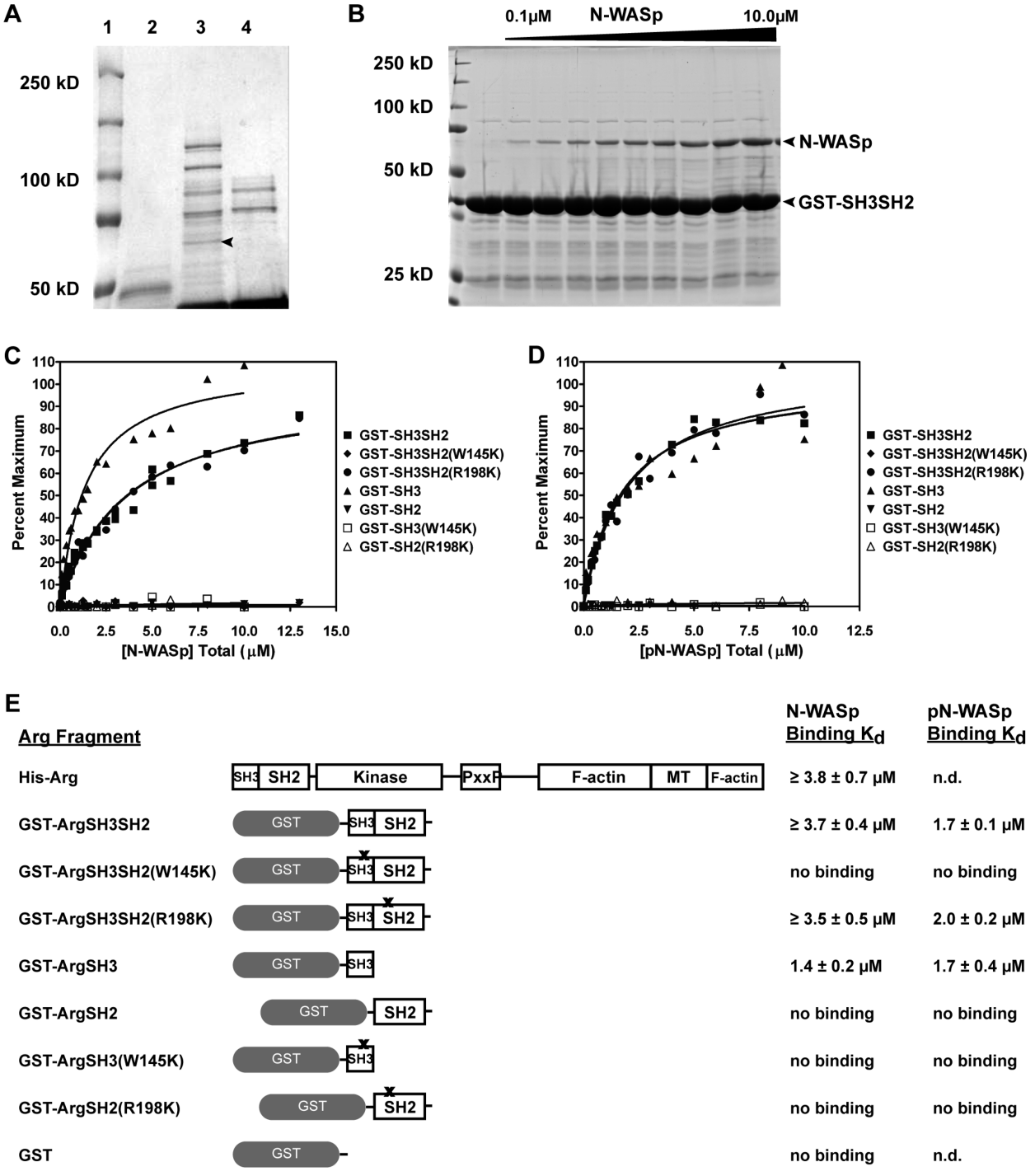

E

Arg Fragment		N-WASp Binding K_d	pN-WASp Binding K_d
His-Arg	SH3 SH2 Kinase PxxP F-actin MT F-actin	≥ 3.8 ± 0.7 μM	n.d.
GST-ArgSH3SH2	GST SH3 SH2	≥ 3.7 ± 0.4 μM	1.7 ± 0.1 μM
GST-ArgSH3SH2(W145K)	GST SH3 SH2	no binding	no binding
GST-ArgSH3SH2(R198K)	GST SH3 SH2	≥ 3.5 ± 0.5 μM	2.0 ± 0.2 μM
GST-ArgSH3	GST SH3	1.4 ± 0.2 μM	1.7 ± 0.4 μM
GST-ArgSH2	GST SH2	no binding	no binding
GST-ArgSH3(W145K)	GST SH3	no binding	no binding
GST-ArgSH2(R198K)	GST SH2	no binding	no binding
GST	GST	no binding	n.d.

FIGURE 1: Arg binds directly to the actin nucleation promoting factor N-WASp. (A) Identification of N-WASp as a GST-Arg-SH3SH2 domain-binding protein. Proteins pulled down from mouse whole brain extracts were visualized by SDS−PAGE followed by Coomassie staining: lane 1, standards; lane 2, proteins pulled down by GST control beads; lane 3, proteins pulled down by GST-Arg-SH3SH2 beads; lane 4, GST-Arg-SH3SH2 beads alone (not exposed to extract). The arrowhead indicates the band identified as N-WASp by mass spectrometry. The two-higher molecular mass bands in lane 4 represent contaminating proteins present in early preps of GST-Arg-SH3SH2, but panel B demonstrates that these contaminants are not essential for Arg−N-WASp binding. (B−E) Mapping interactions between N-WASp and Arg. Arg or Arg fragments were immobilized on beads and incubated with a range of concentrations of N-WASp or phosphorylated N-WASp (pN-WASp) to measure binding affinities (K_d). (B) Representative binding assay gel showing binding of immobilized GST-Arg-SH3SH2 to increasing concentrations of soluble N-WASp. (C and D) Quantitation of binding between GST fusion Arg fragments and N-WASp or pN-WASp. Data were normalized to 100% at maximum binding, which was determined from the plateau of the best-fit binding isotherm. Data were fit to binding isotherms to determine K_d values using GraphPad Prism. (E) Table depicting Arg and Arg fragments used in N-WASp and pN-WASp binding experiments, Arg fragment domain structures, and K_d values of each interaction. In cases where the highest concentration tested was not greater than 10 times the determined K_d, the K_d values are reported as lower limits.

mCherry-tagged N-WASp. Cells were plated on glass coverslips coated with 1 μg/mL fibronectin. Cells were fixed and imaged as previously described (*8*).

Time-Lapse Microscopy and Kymography. Time-lapse microscopy and kymography were performed as previously described (*8*, *13*). Briefly, cells were plated on fibronectin-coated

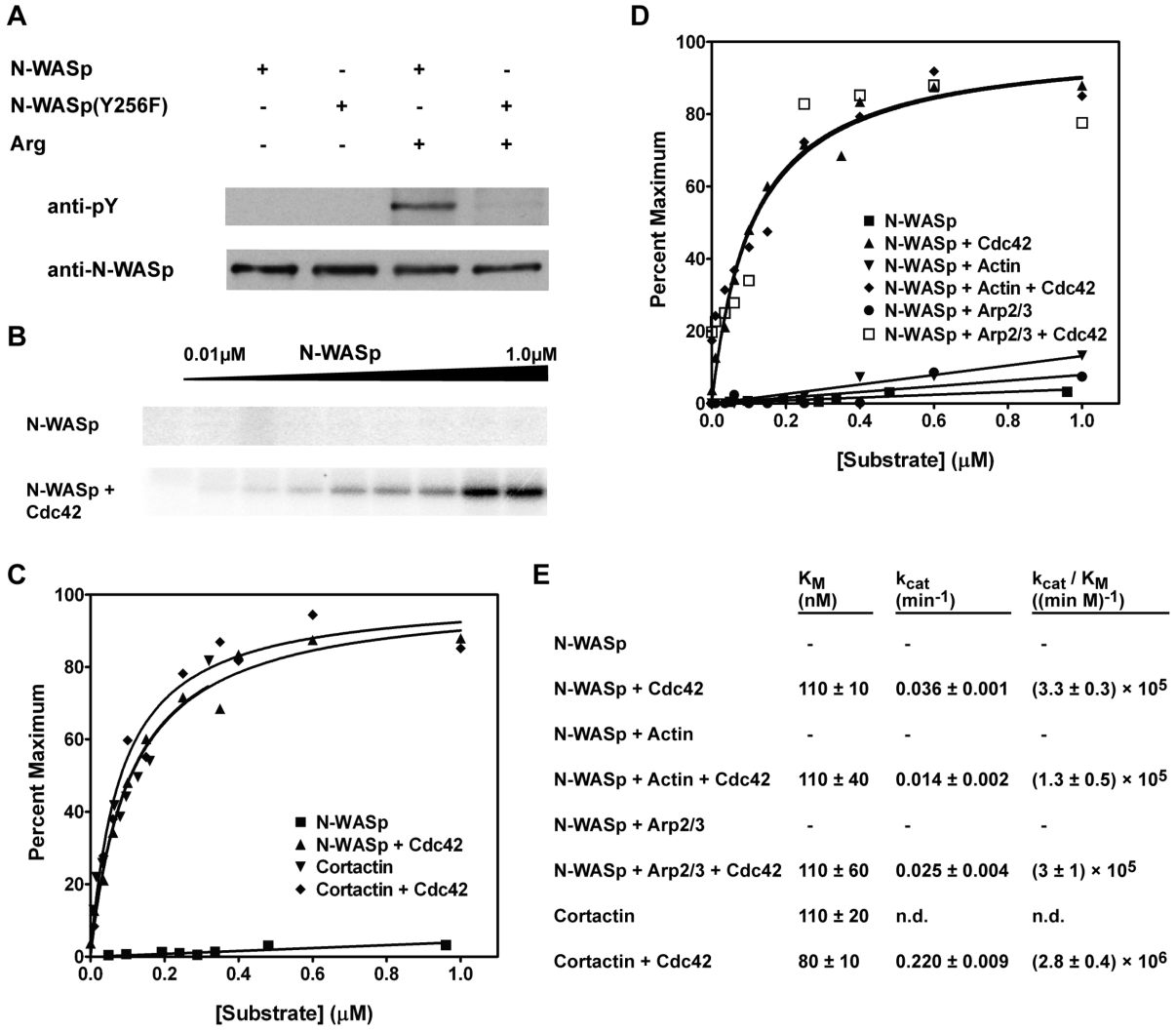

E

	K_M (nM)	k_{cat} (min^{-1})	k_{cat}/K_M ($(min\ M)^{-1}$)
N-WASp	-	-	-
N-WASp + Cdc42	110 ± 10	0.036 ± 0.001	$(3.3 \pm 0.3) \times 10^5$
N-WASp + Actin	-	-	-
N-WASp + Actin + Cdc42	110 ± 40	0.014 ± 0.002	$(1.3 \pm 0.5) \times 10^5$
N-WASp + Arp2/3	-	-	-
N-WASp + Arp2/3 + Cdc42	110 ± 60	0.025 ± 0.004	$(3 \pm 1) \times 10^5$
Cortactin	110 ± 20	n.d.	n.d.
Cortactin + Cdc42	80 ± 10	0.220 ± 0.009	$(2.8 \pm 0.4) \times 10^6$

FIGURE 2: Arg phosphorylates N-WASp on Y256F. (A) His_6-N-WASp or His_6-N-WASp(Y256F) was expressed alone or co-expressed with (untagged) Arg in insect cells as indicated. N-WASp species were purified over a Ni affinity column, and 30 ng of purified protein was immunoblotted with anti-phosphotyrosine antibodies (anti-pY, top) or N-WASp antibodies (bottom). N-WASp with the Y256F substitution was not phosphorylated in insect cells. (B) Cdc42 is required for Arg to phosphorylate N-WASp. Purified recombinant N-WASp (0.01−1.0 μM) was incubated in kinase buffer [25 mM HEPES (pH 7.25), 5% glycerol, 100 mM NaCl, 1 mM $NaVO_4$, and 20 μg/mL BSA] at 30 °C with 10 nM Arg in the presence of Mg^{2+} or Mn^{2+} and [γ-^{32}P]ATP, with or without 7 μM constitutively active GST-Cdc42(G12V), for 5 min. Phosphorimages of representative kinase assays show phosphorylation of N-WASp by Arg in the absence or presence of GST-Cdc42(G12V). (C) Cdc42 stimulates phosphorylation of N-WASp by Arg. Phosphorylation of a range of concentrations of N-WASp or cortactin by Arg in the absence or presence of 5.7 μM GST-Cdc42(G12V). Arg requires GST-Cdc42(G12V) to phosphorylate N-WASp but not cortactin. (D) Effects on Arg-dependent phosphorylation of N-WASp by combinations of 3 μM actin, 10 nM Arp2/3 complex, and 5.7 μM GST-Cdc42(G12V). (E) Data from panels C and D fitted to the Michaelis−Menten equation to determine K_M and k_{cat} values. Dashes represent values that were too high or too low to measure.

coverslips (1 μg/mL) and imaged from 30 min to 2 h postplating. Images were collected every 10 s for a period of 10 min. Kymography was performed using ImageJ (National Institutes of Health, Bethesda, MD), and statistical analysis of cell edge dynamics data was performed using analysis of variance (ANOVA) with StatView (SAS Institute).

RESULTS

Identification of N-WASp as an Arg-Interacting Protein in Mouse Brain Extract. Arg contains an SH3 domain and an SH2 domain upstream of its kinase domain. We used a recombinant protein fragment consisting of glutathione *S*-transferase (GST) fused to this SH3SH2 region of Arg (GST-Arg-SH3SH2) to affinity purify interacting proteins from extracts of whole mouse brains. Several proteins bind to GST-Arg-SH3SH2 beads but not to control GST beads (Figure 1A). Mass spectrometry of the proteins identified the band running at 65 kDa as N-WASp, a ubiquitously expressed nucleation promoting factor that binds the Arp2/3 complex and stimulates its ability to nucleate actin polymerization (*2*). This finding suggested that N-WASp might be part of a pathway coupling Arg to the formation of actin-based protrusions.

The Arg SH3 Domain Mediates Direct Binding to N-WASp. Purified recombinant His_6-tagged N-WASp binds to beads coated with GST-Arg-SH3SH2 in a concentration-dependent manner with a K_d of $\geq 3.7 \pm 0.4$ μM (Figure 1B,C). This affinity is a lower limit based on the highest concentration of N-WASp that could be achieved in the reaction, which was not 10 times the K_d. Similar results were obtained when the binding assay was also conducted by measuring the amount of N-WASp depleted from the supernatant (data not shown), indicating that the off rate of this interaction is slow and validating the results of

the pull-down method. N-WASp binds with a similar affinity to full-length Arg ($K_d \geq 3.8 \pm 0.7\ \mu M$) (Figure 1E), suggesting that the Arg SH3SH2 region alone mediates binding to N-WASp. N-WASp does not bind appreciably to GST alone. The Arg GST-SH3 domain binds N-WASp with a higher affinity ($K_d = 1.4 \pm 0.2\ \mu M$) than the GST-Arg-SH3SH2 domain, but the Arg GST-SH2 domain does not detectably bind N-WASp (Figure 1C,E). GST-Arg-SH3SH2 with a binding-defective point mutation in the SH3 domain (W145K) fails to bind N-WASp, while a binding-defective mutation in the SH2 domain (R198K) does not affect the affinity of GST-Arg-SH3SH2 for N-WASp (Figure 1C,E). These observations show that the Arg SH3 domain is necessary and sufficient to bind N-WASp. Consistent with these findings, SH3 domains bind to proline-rich regions with P-x-x-P motifs (*23*), and N-WASp contains an extensive proline-rich region, including several P-x-x-P motifs, known to bind SH3 domains of other proteins (*24*−*27*). The low micromolar affinity of Arg-SH3 for N-WASP is similar to the affinities of other SH3 domains for P-x-x-P motifs (*28*−*30*).

Arg Phosphorylates N-WASp on Y256. Phosphorylation of N-WASp on Y256 potentiates its ability to stimulate actin nucleation by the Arp2/3 complex (*31*−*33*), and the Arg paralog Abl phosphorylates N-WASp at Y256 (*34*). N-WASp is heavily tyrosine phosphorylated when co-overexpressed in insect cells with Arg but not when it is expressed alone (Figure 2A). N-WASp(Y256F) is not tyrosine phosphorylated when co-overexpressed with Arg, strongly suggesting that Y256 is the primary site of Arg-mediated N-WASp phosphorylation. Purified recombinant Arg phosphorylates purified recombinant N-WASp with a K_M of 110 ± 10 nM (Figure 2B−E), similar to other substrates of Arg (*6*, *9*, *17*). In addition, Arg phosphorylates N-WASp with a k_{cat} of $0.036 \pm 0.001\ min^{-1}$ and a catalytic efficiency k_{cat}/K_M of $(3.3 \pm 0.3) \times 10^5\ min^{-1}\ M^{-1}$ (Figure 2E), values that are both within the range of known physiological Arg substrate concentrations (*12*, *17*). Consistent with previous reports of N-WASp tyrosine phosphorylation, robust in vitro phosphorylation of N-WASp by Arg is observed only in the presence of an N-WASp binding partner capable of keeping N-WASp in its open state, in this case constitutively active GST-Cdc42(G12V) (*33*, *34*). GST-Cdc42(G12V) does not directly influence Arg kinase activity, as Arg had a similar K_M for cortactin in the presence and absence of GST-Cdc42(G12V) (Figure 2C,E), similar to the K_M that we reported previously (*9*). Because Arg and N-WASp both bind actin and because N-WASp interacts with the Arp2/3 complex (*22*, *35*), we also investigated whether actin or the Arp2/3 complex could stimulate Arg phosphorylation of N-WASp, both in the presence and in the absence of GST-Cdc42(G12V). Neither actin (3 μM) nor the Arp2/3 complex (10 nM) stimulates N-WASp phosphorylation by Arg, either in the presence or in the absence of added GST-Cdc42(G12V) (Figure 2D,E).

Arg Binds Phosphorylated N-WASp with Higher Affinity. SH2 domains bind to phosphotyrosine residues, so we examined whether phosphorylation of N-WASp by Arg might create an additional binding site for the SH2 domain of Arg. The affinity of GST-Arg-SH3SH2 for pN-WASp is higher ($1.7 \pm 0.1\ \mu M$) than for nonphosphorylated N-WASp ($\geq 3.7 \pm 0.1\ \mu M$) (Figure 1E) and similar to the affinities of Arg GST-SH3 for phosphorylated or unphosphorylated N-WASp. Interestingly, the SH3 mutation (W145K) completely abrogates binding of GST-Arg-SH3SH2 to pN-WASp, while the SH2 mutation (R198K) does not affect the affinity of GST-Arg-SH3SH2 for pN-WASp (Figure 1D,E). This observation suggests the higher affinity of GST-Arg-SH3SH2 for pN-WASp is not due to a new SH2−phosphotyrosine interaction, but rather to an increased affinity of the Arg SH3 domain for pN-WASp. The increased affinity of the tested Arg fragments for pN-WASp may indicate that N-WASp phosphorylation

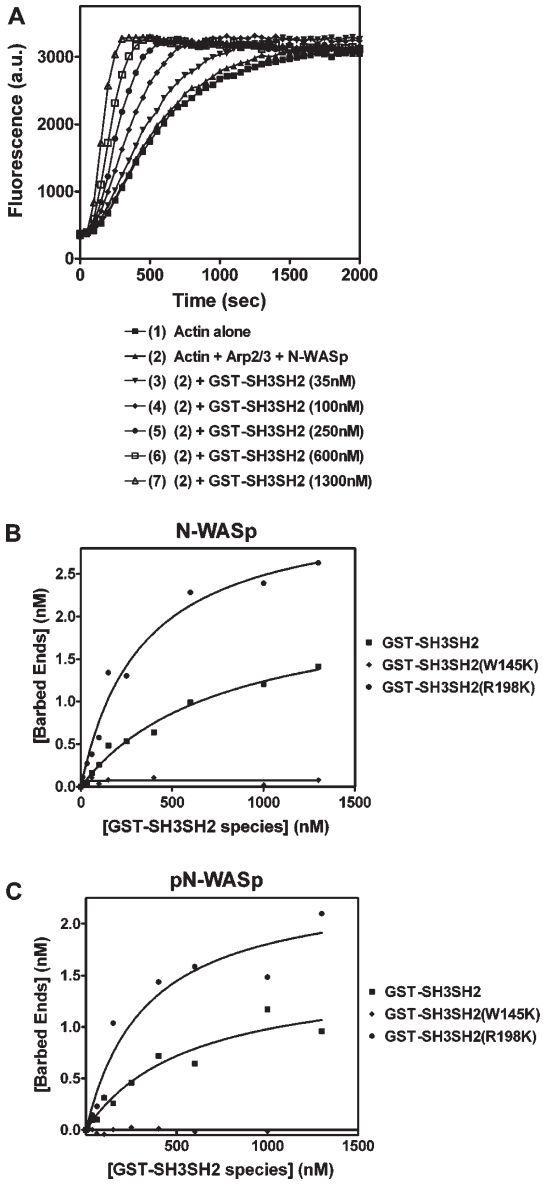

FIGURE 3: GST-Arg-SH3SH2 stimulates actin polymerization by N-WASp and the Arp2/3 complex. (A) Time course of actin polymerization with N-WASp, the Arp2/3 complex, and a range of concentrations of GST-Arg-SH3SH2. Conditions: modified KMEI buffer [63 mM KCl, 1 mM $MgCl_2$, 1 mM EGTA, and 19 mM imidazole (pH 7.0)] at 25 °C, 3 μM actin monomers, with or without 10 nM Arp2/3 complex, with or without 4 nM N-WASp and 0−1.3 μM GST-Arg-SH3SH2. N-WASp was strongly autoinhibited, because it had no effect on the time course of polymerization compared with actin alone or actin with the Arp2/3 complex. GST-Arg-SH3SH2 accelerated the time course of polymerization in a concentration-dependent fashion. (B and C) Dependence of the number of actin filament barbed ends produced by 10 nM Arp2/3 complex and 4 nM N-WASP on the concentration of GST-Arg-SH3SH2 domain constructs. The number of filaments was calculated from the rate of polymerization when 80% of the actin monomers had been consumed (*22*): (B) unphosphorylated N-WASp and (C) phosphorylated N-WASp. GST-Arg-SH3SH2 activates N-WASp and pN-WASp similarly. GST-Arg-SH3SH2(R198K) is activated in a manner similar to that of the wild type, but GST-Arg-SH3SH2(W145K) does not activate either N-WASp species.

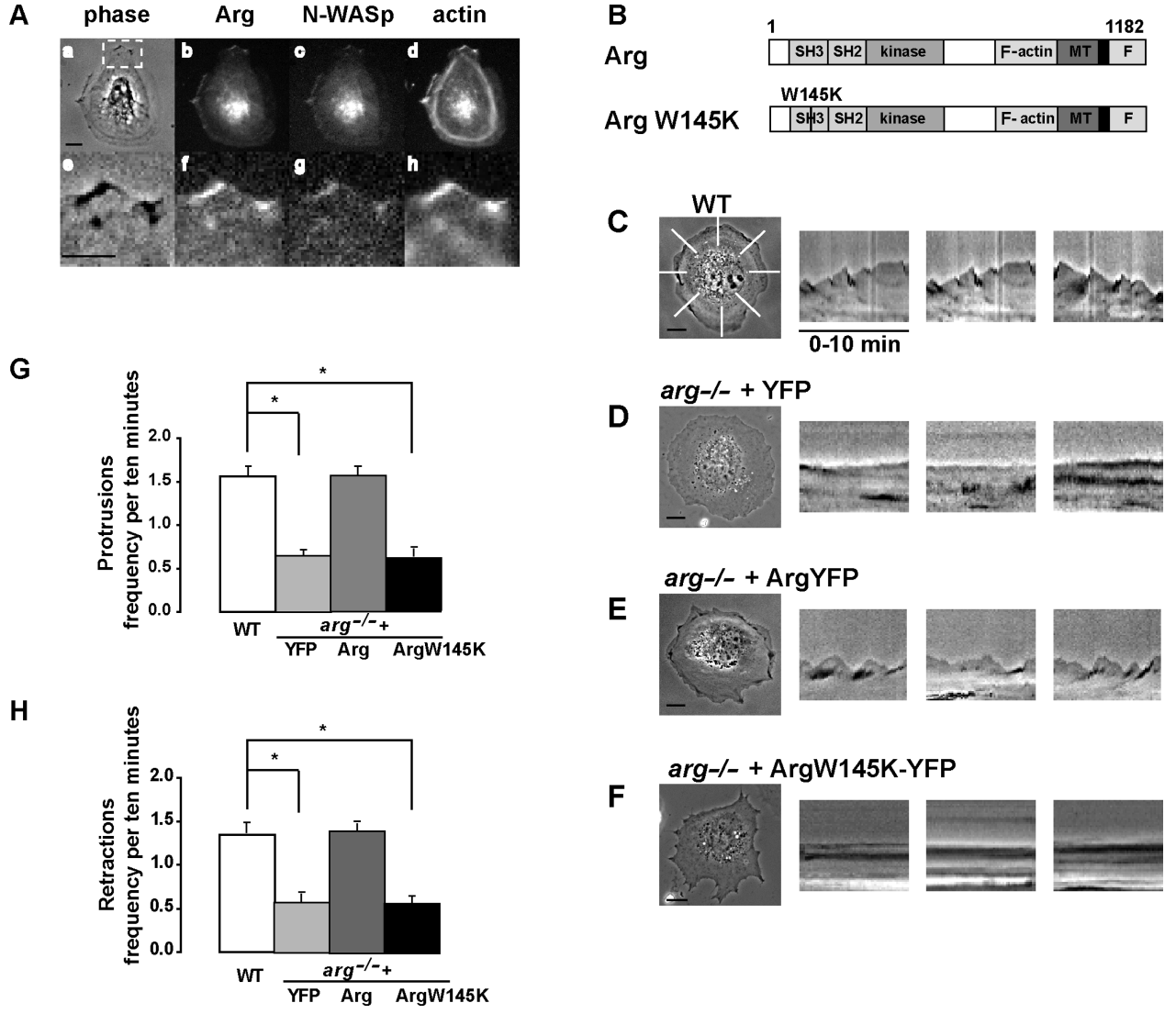

FIGURE 4: Arg and N-WASp colocalize to cell edge protrusions, and the Arg SH3 domain is required for efficient adhesion-dependent cell edge dynamics. (A) Arg-YFP and mCherry-N-WASp colocalize to actin-rich cell edge protrusions when co-expressed in *arg*−/− cells. Panels E−H are enlargements of the region boxed in panel A. (B) Graphical depiction of full-length Arg and the ArgW145K mutant used in this experiment. Arg contains SH3, SH2, and kinase domains at its N-terminus. The C-terminus of Arg contains a proline (P)-rich region, two F-actin, and a microtubule (MT) binding site. (C−F) Representative images taken from a 10 min time-lapse video. Kymographs were recorded at eight different positions as indicated in panel C, and three representative kymographs for each cell are presented: (C) WT cells (n = 20 cells), (D) *arg*−/− cells (n = 22 cells), (E) *arg*−/− cells expressing Arg-YFP (n = 34 cells), and (F) *arg*−/− cells expressing ArgW145K-YFP (n = 34 cells). (G and H) Quantification of cell edge protrusions (G) and retractions (H). Values are means ± the standard error of the mean. ANOVA between all cell types: protrusions, $P < 0.0001$; retractions, $P < 0.0001$. Fisher's PLSD for all cells versus *arg*−/−: $^*P < 0.01$. Bars are 10 μm.

alters its conformation to allow tighter binding of Arg fragments (see the Discussion).

Arg Stimulates N-WASp-Dependent Actin Polymerization in Vitro. We used fluorescence enhancement of pyrenyl-actin to measure the ability of Arg fragments, N-WASp, and pN-WASp to stimulate actin polymerization by the Arp2/3 complex. Actin alone polymerizes slowly after an initial lag (Figure 3A). The Arp2/3 complex with or without N-WASp does not stimulate polymerization, showing that our N-WASp preparation is fully autoinhibited. Consistent with previous reports (*31*−*33*), pN-WASp is slightly more active than N-WASp at high concentrations, suggesting that pN-WASp is less autoinhibited (data not shown). GST-Arg-SH3SH2 stimulates actin polymerization with the Arp2/3 complex and N-WASp or pN-WASp in a concentration-dependent manner by reducing the initial lag and increasing the maximum rate of polymerization (Figure 3A,B). GST-Arg-SH3SH2 stimulates N-WASp and pN-WASp with similar potency in spite of the higher affinity of GST-Arg-SH3SH2 for pN-WASp (Figure 3C). The SH3 binding-defective GST-Arg-SH3SH2(W145K) mutant does not stimulate actin nucleation by N-WASp or pN-WASp and the Arp2/3 complex. In contrast, mutation of the SH2 domain has no effect on the ability of GST-Arg-SH3SH2 to stimulate actin nucleation (Figure 3B). These results indicate that Arg uses its SH3 domain to bind to and activate N-WASp and pN-WASp, thereby promoting their interaction with the Arp2/3 complex and stimulating actin polymerization. The difference in activation plateaus of GST-Arg-SH3SH2 and GST-Arg-SH3SH2(R198K) likely reflects the different specific activities of the protein samples.

Arg and N-WASp Colocalize to Adhesion-Dependent Cell Edge Protrusions. We previously showed that adhesion of fibroblasts to fibronectin stimulates localization of Arg to the cell periphery, where it promotes dynamic adhesion-dependent cell edge protrusions (*8*, *13*, *35*). To test whether Arg might interact

with N-WASp to mediate these protrusions, we co-expressed Arg-YFP and mCherry-N-WASp in *arg*−/− fibroblasts and monitored their localization during fibroblast adhesion and spreading on fibronectin-coated coverslips. Arg-YFP and mCherry-N-WASp colocalize to actin-rich protrusive structures at the cell periphery when plated on fibronectin-coated coverslips (Figure 4 A), consistent with a possible role for Arg−N-WASp interactions in mediating adhesion-dependent cell edge protrusions.

An Arg Mutant Defective for N-WASp Binding Does Not Support Cell Edge Protrusion. Wild-type (WT) fibroblasts exhibit robust dynamic cell edge protrusion during adhesion to fibronectin-coated surfaces. Kymographs of the cell edge reveal a "rolling hill" profile that reflects these dynamic protrusions and retractions (*8*, *13*) (see also Figure 4C,G,H). In contrast, *arg*−/− fibroblasts exhibit significant deficits in adhesion-dependent cell edge protrusion, yielding flat "prairie"-like kymographs (*8*, *13*) (see also Figure 4 D,G,H). Retroviral-mediated re-expression of Arg-YFP in *arg*−/− fibroblasts restores adhesion-dependent cell edge protrusion to those of WT fibroblasts (Figure 4E,G,H), as we have shown previously (*8*, *13*). In contrast, retroviral-mediated re-expression of the SH3 point mutant defective in binding N-WASp (ArgW145K-YFP) was unable to complement the protrusion deficits of *arg*−/− cells (Figure 4B,F,G,H). Together with the colocalization studies, these data suggest that Arg:N-WASp interactions are important for efficient adhesion-dependent cell edge protrusion.

DISCUSSION

Arg interacts with N-WASp through both binding and phosphorylation events. These interactions allow Arg to regulate N-WASp function and provide a direct pathway through which Arg can regulate actin polymerization.

Direct Interaction of Arg and N-WASp: Binding and Phosphorylation. We show that Arg interacts with N-WASp in two ways. First, the Arg SH3 domain binds N-WASp, presumably to a P-x-x-P motif. Second, Arg phosphorylates N-WASp with a K_M similar to those of other endogenous substrates of Arg. This is the second example of multimodal interaction between Arg and an actin-binding protein. The SH3 domain of cortactin binds an Arg P-x-x-P motif, and this interaction is strengthened by an interaction between the Arg SH2 domain and phosphotyrosine residues on cortactin subsequent to Arg phosphorylation of cortactin (*9*, *13*). We hypothesized that the Arg SH2 domain might bind phosphorylated N-WASp similarly, but this turned out not to be the case.

We observed two levels of binding affinity between the Arg SH3 and SH2 constructs and N-WASp. The isolated SH3 domain bound pN-WASp and N-WASp with the same high affinity, but all of the larger Arg constructs containing both the SH3 and SH2 domains had a lower affinity for N-WASp than pN-WASp. Steric hindrance due to the added bulk of the Arg SH2 domain and the closed conformation of unphosphorylated N-WASp may explain why the affinity of the Arg SH3 domain for the P-x-x-P binding site in N-WASp is decreased. With both of these steric factors present, interaction of the SH3 domain and P-x-x-P site is weakened, but full binding affinity is restored when either of these factors is removed, either by deletion of the SH2 domain or by opening of the N-WASp conformation through phosphorylation.

Steric interactions are also important in regulating the accessibility of N-WASp to the kinase domain of Arg. Binding partners that release WASp family proteins from their autoinhibited, conformationally closed state make them better substrates for tyrosine kinases by exposing a buried tyrosine that is the target of these kinases (*33*, *34*). Although stoichiometric concentrations of GST-Arg-SH3SH2 activate N-WASP, low, catalytic concentrations of Arg are unable to phosphorylate autoinhibited N-WASp. However, in the presence of an excess of GST-Cdc42(G12V), a constitutively active Rho family GTPase known to bind to and open N-WASp, Arg phosphorylates N-WASp with a K_M similar to those of other Arg substrates.

Regulation of N-WASp-Dependent Actin Polymerization by Arg. Consistent with our binding data showing that the Arg SH3 domain binds N-WASp, we find that the Arg SH3 domain also activates N-WASp to promote actin polymerization by the Arp2/3 complex. The SH3 domains of other proteins, including Nck and Grb2, also stimulate N-WASp (*25*, *26*). Torres and Rosen proposed that once opened by Cdc42 binding, phosphorylation keeps WASP or N-WASp in an active configuration, a form of "molecular memory" (*33*). We find that Arg-SH3SH2 binding is sufficient to activate N-WASp, or phospho-N-WASp, even in the absence of Cdc42. This Arg-dependent activation may represent a novel activation mode in which Arg-SH3SH2 binding, rather than phosphorylation, keeps N-WASp open.

Dimers of WASp family constructs are much more active NPFs than monomeric constructs (*22*) because of their ability to occupy both NPF binding sites on the Arp2/3 complex (*36*). GST-induced dimerization presumably contributes to the ability of proteins with two SH3 domains such as our GST-Arg-SH3 constructs to activate N-WASp (*36*). Although full-length Arg contains only one SH3 domain, Arg binds cooperatively to actin filaments, which promotes clustering of Arg on actin filaments in vitro and likely helps concentrate Arg within protrusive structures in cells (*8*, *35*). In this manner, two adjacent Arg molecules, cross-linked by actin filaments, may act as a functional unit with two SH3 domains to efficiently activate N-WASp. In addition, since Arg contains multiple protein−protein interaction domains, Arg likely further facilitates N-WASp stimulation by putting it in the proximity of its other binding partners, including actin filaments, cortactin, and the Nck adaptor protein.

Our in vitro experiments describe a mechanism by which Arg regulates actin polymerization through interaction with N-WASp. We also show that Arg and N-WASp colocalize at the cell periphery in response to adhesive cues. The Arg SH3 domain, which mediates binding of Arg to N-WASp, is required for this adhesion-dependent protrusion, pointing to this interaction as a mechanism through which Arg mediates stimulus-dependent actin-based protrusion. We propose a model in which Arg and cortactin weakly associate at the cell periphery until PDGF or integrin signaling activates Arg to phosphorylate both cortactin and N-WASp. These phosphorylation events facilitate binding of Arg to phosphorylated cortactin via its SH2 domain (*13*) and pN-WASp via its SH3 domain. In this way, Arg may act in a scaffolding capacity, bringing cortactin and N-WASp together in close proximity to each other and allowing them to bind to each other, the Arp2/3 complex, the actin filament, and an actin monomer, thereby initiating the actin polymerization to drive cell edge protrusion.

ACKNOWLEDGMENT

We thank Xianyun Ye and Hongli Chen for technical assistance; S. Boyle, B. Bradley, R. Mahaffy, B. Nolen, and A. Paul

for experimental advice; B. Bradley, B. Couch, C. Mader, and D. Wetzel for critical comments on the manuscript; and members of the Koleske lab and Pollard lab for helpful discussions and feedback. M.M.M. created expression constructs and performed the biochemistry. S.L. performed Arg and N-WASp localization experiments and kymographic analysis of cell edge behavior. M.M.M. and S.M.M. performed in vitro kinase assays. M.K.S. conducted pull downs from brain extract and identified N-WASp, and A.J.K. created expression constructs and cell lines in A.J.K.'s laboratory. M.M.M. purified actin and the Arp2/3 complex and performed actin polymerization assays in T.D.P.'s laboratory. M.M.M. and A.J.K. wrote the manuscript, and all others edited. T.D.P. also provided guidance on the design and interpretation of experiments.

REFERENCES

1. Ismail, A. M., Padrick, S. B., Chen, B., Umetani, J., and Rosen, M. K. (2009) The WAVE regulatory complex is inhibited. *Nat. Struct. Mol. Biol. 16*, 561–563.
2. Rohatgi, R., Ma, L., Miki, H., Lopez, M., Kirchhausen, T., Takenawa, T., and Kirschner, M. W. (1999) The interaction between N-WASP and the Arp2/3 complex links Cdc42-dependent signals to actin assembly. *Cell 97*, 221–231.
3. Rouiller, I., Xu, X.-P., Amann, K. J., Egile, C., Nickell, S., Nicastro, D., Li, R., Pollard, T. D., Volkmann, N., and Hanein, D. (2008) The structural basis of actin filament branching by the Arp2/3 complex. *J. Cell Biol. 180*, 887–895.
4. Mullins, R. D., Heuser, J. A., and Pollard, T. D. (1998) The interaction of Arp2/3 complex with actin: Nucleation, high affinity pointed end capping, and formation of branching networks of filaments. *Proc. Natl. Acad. Sci. U.S.A. 95*, 6181–6186.
5. Svitkina, T. M., and Borisy, G. G. (1999) Arp2/3 complex and actin depolymerizing factor/cofilin in dendritic organization and treadmilling of actin filament array in lamellipodia. *J. Cell Biol. 145*, 1009–1026.
6. Hernandez, S. E., Settleman, J., and Koleske, A. J. (2004) Adhesion-dependent regulation of p190RhoGAP in the developing brain by the Abl-related gene tyrosine kinase. *Curr. Biol. 14*, 691–696.
7. Moresco, E. M. Y., Donaldson, S., Williamson, A., and Koleske, A. J. (2005) Integrin-mediated dendrite branch maintenance requires Abelson (Abl) family kinases. *J. Neurosci. 25*, 6105–6118.
8. Miller, A. L., Wang, Y., Mooseker, M. S., and Koleske, A. J. (2004) The Abl-related gene (Arg) requires its F-actin-microtubule cross-linking activity to regulate lamellipodial dynamics during fibroblast adhesion. *J. Cell Biol. 165*, 407–419.
9. Boyle, S. N., Michaud, G. A., Schweitzer, B., Predki, P. F., and Koleske, A. J. (2007) A critical role for cortactin phosphorylation by Abl-family kinases in PDGF-induced dorsal-wave formation. *Curr. Biol. 17*, 445–451.
10. Plattner, R., Koleske, A. J., Kazlauskas, A., and Pendergast, A. M. (2004) Bidirectional signaling links the Abelson kinases to the platelet-derived growth factor receptor. *Mol. Cell. Biol. 24*, 2573–2583.
11. Bradley, W. D., Hernandez, S. E., Settleman, J., and Koleske, A. J. (2006) Integrin signaling through Arg activates p190RhoGAP by promoting its binding to p120RasGAP and recruitment to the membrane. *Mol. Biol. Cell 17*, 4827–4836.
12. Boyle, S. N., and Koleske, A. J. (2007) Use of a chemical genetic technique to identify myosin IIb as a substrate of the Abl-related gene (Arg) tyrosine kinase. *Biochemistry 46*, 11614–11620.
13. Lapetina, S., Mader, C. C., Machida, K., Mayer, B. J., and Koleske, A. J. (2009) Arg interacts with cortactin to promote adhesion-dependent cell edge protrusion. *J. Cell Biol. 185*, 503–519.
14. Miki, H., Miura, K., and Takenawa, T. (1996) N-WASP, a novel actin-depolymerizing protein, regulates the cortical cytoskeletal rearrangement in a PIP2-dependent manner downstream of tyrosine kinases. *EMBO J. 15*, 5326–5335.
15. Laemmli, U. K. (1970) Cleavage of structural proteins during the assembly of the head of bacteriophage T4. *Nature 227*, 680–685.
16. Sfakianos, M. K., Wilson, L., Sakalian, M., Falany, C. N., and Barnes, S. (2002) Conserved residues in the putative catalytic triad of human bile acid Coenzyme A:amino acid N-acyltransferase. *J. Biol. Chem. 277*, 47270–47275.
17. Tanis, K. Q., Veach, D., Duewel, H. S., Bornmann, W. G., and Koleske, A. J. (2003) Two distinct phosphorylation pathways have additive effects on Abl family kinase activation. *Mol. Cell. Biol. 23*, 3884–3896.
18. Mahaffy, R. E., and Pollard, T. D. (2006) Kinetics of the formation and dissociation of actin filament branches mediated by Arp2/3 complex. *Biophys. J. 91*, 3519–3528.
19. Spudich, J. A., and Watt, S. (1971) The regulation of rabbit skeletal muscle contraction. I. Biochemical studies of the interaction of the tropomyosin-troponin complex with actin and the proteolytic fragments of myosin. *J. Biol. Chem. 246*, 4866–4871.
20. Pollard, T. D. (1984) Polymerization of ADP-actin. *J. Cell Biol. 99*, 769–777.
21. Cooper, J. A., Walker, S. B., and Pollard, T. D. (1983) Pyrene actin: Documentation of the validity of a sensitive assay for actin polymerization. *J. Muscle Res. Cell Motil. 4*, 253–262.
22. Higgs, H. N., Blanchoin, L., and Pollard, T. D. (1999) Influence of the C terminus of Wiskott-Aldrich syndrome protein (WASp) and the Arp2/3 complex on actin polymerization. *Biochemistry 38*, 15212–15222.
23. Ren, R., Mayer, B. J., Cicchetti, P., and Baltimore, D. (1993) Identification of a ten-amino acid proline-rich SH3 binding site. *Science 259*, 1157–1161.
24. Fukuoka, M., Suetsugu, S., Miki, H., Fukami, K., Endo, T., and Takenawa, T. (2001) A novel neural Wiskott-Aldrich syndrome protein (N-WASP) binding protein, WISH, induces Arp2/3 complex activation independent of Cdc42. *J. Cell Biol. 152*, 471–482.
25. Carlier, M. F., Nioche, P., Broutin-L'Hermite, I., Boujemaa, R., Le Clainche, C., Egile, C., Garbay, C., Ducruix, A., Sansonetti, P., and Pantaloni, D. (2000) GRB2 links signaling to actin assembly by enhancing interaction of neural Wiskott-Aldrich syndrome protein (N-WASp) with actin-related protein (ARP2/3) complex. *J. Biol. Chem. 275*, 21946–21952.
26. Rohatgi, R., Nollau, P., Ho, H. Y., Kirschner, M. W., and Mayer, B. J. (2001) Nck and phosphatidylinositol 4,5-bisphosphate synergistically activate actin polymerization through the N-WASP-Arp2/3 pathway. *J. Biol. Chem. 276*, 26448–26452.
27. Ho, H.-Y. H., Rohatgi, R., Lebensohn, A. M., Le, M., Li, J., Gygi, S. P., and Kirschner, M. W. (2004) Toca-1 mediates Cdc42-dependent actin nucleation by activating the N-WASP-WIP complex. *Cell 118*, 203–216.
28. Chen, J. K., Lane, W. S., Brauer, A. W., Tanaka, A., and Schreiber, S. L. (1993) Biased combinatorial libraries: Novel ligands for the SH3 domain of phosphatidylinositol 3-kinase. *J. Am. Chem. Soc. 115*, 12591–12592.
29. Feng, S., Chen, J. K., Yu, H., Simon, J. A., and Schreiber, S. L. (1994) Two binding orientations for peptides to the Src SH3 domain: Development of a general model for SH3-ligand interactions. *Science 266*, 1241–1247.
30. Yu, H., Chen, J. K., Feng, S., Dalgarno, D. C., Brauer, A. W., and Schreiber, S. L. (1994) Structural basis for the binding of proline-rich peptides to SH3 domains. *Cell 76*, 933–945.
31. Suetsugu, S., Hattori, M., Miki, H., Tezuka, T., Yamamoto, T., Mikoshiba, K., and Takenawa, T. (2002) Sustained activation of N-WASP through phosphorylation is essential for neurite extension. *Dev. Cell 3*, 645–658.
32. Cory, G. O. C., Garg, R., Cramer, R., and Ridley, A. J. (2002) Phosphorylation of tyrosine 291 enhances the ability of WASp to stimulate actin polymerization and filopodium formation. Wiskott-Aldrich Syndrome protein. *J. Biol. Chem. 277*, 45115–45121.
33. Torres, E., and Rosen, M. K. (2003) Contingent phosphorylation/dephosphorylation provides a mechanism of molecular memory in WASP. *Mol. Cell 11*, 1215–1227.
34. Burton, E. A., Oliver, T. N., and Pendergast, A. M. (2005) Abl kinases regulate actin comet tail elongation via an N-WASP-dependent pathway. *Mol. Cell. Biol. 25*, 8834–8843.
35. Wang, Y., Miller, A. L., Mooseker, M. S., and Koleske, A. J. (2001) The Abl-related gene (Arg) nonreceptor tyrosine kinase uses two F-actin-binding domains to bundle F-actin. *Proc. Natl. Acad. Sci. U. S.A. 98*, 14865–14870.
36. Padrick, S. B., Cheng, H.-C., Ismail, A. M., Panchal, S. C., Doolittle, L. K., Kim, S., Skehan, B. M., Umetani, J., Brautigam, C. A., Leong, J. M., and Rosen, M. K. (2008) Hierarchical regulation of WASP/WAVE proteins. *Mol. Cell 32*, 426–438.